

# QCD thermodynamics with dynamical overlap fermions

Szabolcs Borsányi<sup>a</sup>, Ydalia Delgado<sup>b</sup>, Stephan Dürr<sup>a,c</sup>, Zoltán Fodor<sup>a,c,d</sup>,  
 Sándor D. Katz<sup>d1</sup>, Stefan Krieg<sup>a,c</sup>, Thomas Lippert<sup>a,c</sup>, Dániel Nógrádi<sup>d</sup> and  
 Kálmán K. Szabó<sup>a</sup>

<sup>a</sup>Bergische Universität Wuppertal, D-42119 Wuppertal, Germany

<sup>b</sup>Institut für Physik, Karl-Franzens Universität, Graz, Austria

<sup>c</sup>IAS, Jülich Supercomputing Centre, Forschungszentrum Jülich, D-52425  
 Jülich, Germany

<sup>d</sup>Institute for Theoretical Physics, Eötvös University, H-1117 Budapest,  
 Hungary

---

## Abstract

We study QCD thermodynamics using two flavors of dynamical overlap fermions with quark masses corresponding to a pion mass of 350 MeV. We determine several observables on  $N_t = 6$  and 8 lattices. All our runs are performed with fixed global topology. Our results are compared with staggered ones and a nice agreement is found.

*Keywords:* QCD transition, Lattice QCD

---

## 1. Introduction

At high temperatures the dominant degrees of freedom of strongly interacting matter change from hadrons to quarks and gluons. This transition can be studied using lattice gauge theory. There are various results using different fermion regularizations.

Most of these results [1, 2, 3] use the computationally least expensive staggered discretization which also preserves some of the continuum chiral symmetry. Even though different staggered results seem to agree with each other one should not forget that all these works use the fourth root trick to study  $N_f = 2 + 1$  flavors of quarks. There is still an ongoing debate

---

<sup>1</sup>katz@bodri.elte.hu

in the literature about the correctness of this approach. Furthermore taste symmetry breaking may lead to large discretization errors when using small quark masses, especially at low temperatures.

There are also several results using Wilson fermions [4, 5, 6]. Since Wilson fermions break chiral symmetry explicitly one has to take very fine lattices to study chiral symmetry restoration at finite temperature. Due to the scattering of the low lying eigenvalues of the Wilson-Dirac operator one needs large lattice volumes when going to small pion masses. There are also first results with twisted mass fermions [7].

It seems logical to use chiral fermions to study chiral properties at finite temperature. Even though lattice chiral fermions are computationally much more expensive than the other types of discretization there are results in the literature using domain wall fermions [8] as well as first attempts with overlap fermions [9]. While domain-wall fermions provide exact chiral symmetry only for an infinite extent of the fifth dimension, the overlap formulation [10, 11] has the advantage of exact symmetry on finite four dimensional lattices [12].

In this exploratory Letter we present results using two degenerate flavors of dynamical overlap fermions. We use two lattice resolutions corresponding to  $N_t = 6$  and 8 temporal extents. We determine the temperature dependence of the chiral condensate, the chiral susceptibility, the quark number susceptibility and the Polyakov loop. The results are compared to  $N_f = 2$  staggered data, the details of these simulations are summarized in Appendix B.

## 2. Lattice action and simulation details

The possibility of using the Hybrid Monte Carlo algorithm (HMC) with overlap fermions was first discussed in Reference [13]. The overlap operator was implemented with a multi-shift inverter using the Zolotarev rational approximation [14]. The working of the algorithm was demonstrated on a small thermodynamic study on  $6^3 \cdot 4$  lattices. It was also observed that treating topology changes requires special care during the HMC trajectories. One has to track the lowest lying eigenvalues of the Wilson kernel of the overlap operator. This was studied in detail in References [15, 16, 17]. It was demonstrated in Reference [18] that one can do simulations with a fixed topological charge in several different sectors and it is possible to determine their relative weight. However, even this approach requires a tracking of Wilson eigenvalues. In Reference [19] it was suggested that by adding an extra heavy Wilson

fermion to the action which decouples in the continuum limit, one can disable topological sector changes and at the same time speed up the algorithm significantly. It was also claimed that in the thermodynamic limit physics is independent of the global topology and therefore this approach should give correct results. However, significant power-like finite volume corrections are expected [20, 21]. Here we follow the same approach: we add an extra Wilson fermion to suppress low lying eigenvalues of the Wilson kernel and disable tunneling between different topological sectors. As a further improvement we use smearing in the Wilson kernel. It was observed in [22] that smearing significantly improves the properties of the overlap operator. Furthermore, since smearing decreases the eigenvalue density in the middle of the Wilson spectrum it results in a significant speedup of the algorithm [23].

In the gauge sector we use a tree level Symanzik improved gauge action. The overlap operator can be written as

$$D = \left(m_0 - \frac{m}{2}\right) (1 + \gamma_5 \text{sgn}(H_W)) + m, \quad (1)$$

where  $H_W = \gamma_5 D_W$  is the Hermitian Wilson operator with a negative  $-2 < -m_0 < 0$  mass parameter and  $m$  is the mass of the overlap quark. For the Wilson kernel we use two steps of HEX smearing [24, 25, 26] with smearing parameters of  $\alpha_1 = 0.72$ ,  $\alpha_2 = 0.60$  and  $\alpha_3 = 0.44$ . In order to set  $m_0$  we evaluated the Wilson kernel on quenched configurations with the targeted lattice spacings in this work and located the point which is in the middle between the physical modes and the first doublers. This resulted in  $m_0=1.3$ . The simulations are performed with  $N_f = 2$  flavors.

As suggested in [19] we add two irrelevant terms to the action to suppress low eigenvalues of  $H_W$  and fix topology:

$$S_E = \sum_x \left\{ \bar{\psi}_E(x) D_W(-m_0) \psi_E(x) + \phi^\dagger(x) [D_W(-m_0) + i m_B \gamma_5 \tau_3] \phi(x) \right\}. \quad (2)$$

The first term is the action of two flavors of extra fermions with negative mass  $-m_0$ . The second term, including a two component bosonic field is included to control the effect of the extra fermions. The eigenvalues of  $H_W$  below  $m_B$  are most strongly suppressed. Since both  $m_0$  and  $m_B$  are fixed in lattice units they correspond to infinitely large masses in the continuum limit and both these terms decouple. For the bosonic mass we use  $m_B=0.54$ . Since our lattice action results in a fixed topology we aimed to make simulations with zero topological charge.

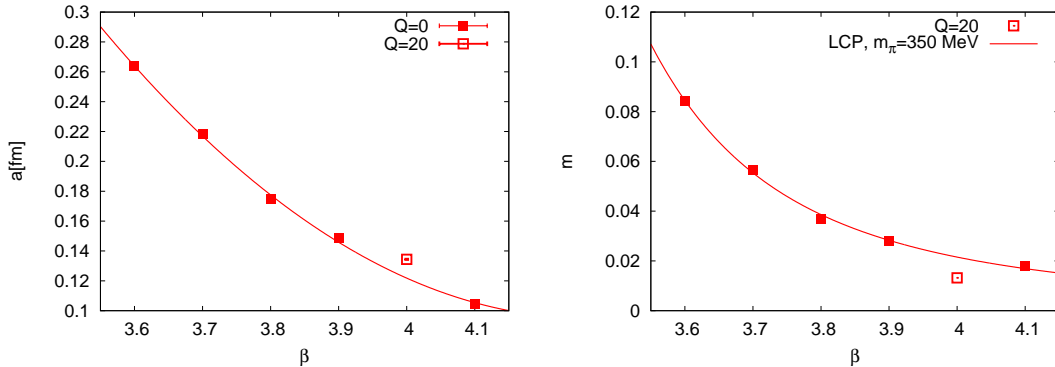


Figure 1: *Left*: The lattice spacing as a function of the  $\beta$  coupling. The opened box shows a run with a fixed topological charge of  $Q = 20$ . *Right*: the bare quark mass as a function of  $\beta$ .

We use a HMC algorithm with the Hasenbusch trick [27], with an Omelyan integrator [28] and with a Sexton-Weingarten multi-scale scheme for the different fields [29]. The latter ingredient turned out to be rather advantageous, the extra Wilson fermion has to be integrated with a much smaller stepsize than the much more expensive overlap fermion.

The first step of our analysis was to determine the line of constant physics (LCP) and the scale. We used  $12^3 \cdot 24$  lattices for  $\beta = 3.6, 3.7, 3.8$  and  $3.9$  and  $16^3 \cdot 32$  for  $\beta = 4.0$  and  $4.1$  with some initial guesses of the bare quark masses between 0.02 and 0.06. We determined the  $w_0$  scale [30] as well as the pion masses on all of these lattices. The  $w_0$  scale is defined implicitly by the equation  $d/dt[t^2 E(t)]|_{t=w_0^2} = 0.3$ , where  $E(t)$  is the expectation value of the gauge action evaluated on configurations evolved by the Wilson flow [31] with parameter  $t$ . Since due to the chiral symmetry of overlap fermions  $m_\pi^2 \propto m$  and the  $w_0$  scale is quite insensitive to the quark mass, it was possible to tune the quark masses to have a fixed value of  $m_\pi \cdot w_0 = 0.312$  for each beta without further simulations. With the physical value of  $w_0$  at the  $N_f = 2 + 1$  flavor physical point,  $w_0 = 0.1755$  fm, this would correspond to  $m_\pi = 350$  MeV. Rigorously a conversion into physical units is only well defined in QCD with physical quark masses, so the results in MeV or fm are for orientation only. The lattice spacing as a function of  $\beta$  and the LCP are shown in Figure 1. In one of our runs we had a nonzero topological charge,  $Q = 20$ . One can see from the plot that both the scale and the LCP have still a significant dependence on topology for our volumes.

For the finite temperature runs we use two sets of lattices:  $12^3 \cdot 6$  and  $16^3 \cdot 8$ . Since the lattice spacing and the LCP is quite ambiguous at large lattice spacings and the algorithm performs poorly on coarse lattices we decided not to do  $N_t = 4$  runs. We had 9 different  $\beta$  values for both  $N_t = 6$  and 8 in the range  $\beta = 3.6 \dots 4.1$ . For renormalization we performed runs at the same gauge couplings on  $12^4$  lattices up to  $\beta = 3.7$ , on  $16^4$  lattices up to  $\beta = 4.05$  and on  $24^3 \cdot 32$  at  $\beta = 4.1$ . We collected up to 2000 HMC trajectories for each finite temperature, and around 500 for each zero temperature point.

### 3. Results

The first quantity we study is the *chiral condensate*,  $\bar{\psi}\psi = (T/V)\partial/\partial m \log Z$ . This can be renormalized using the zero temperature condensate  $\bar{\psi}\psi_0$  (this observable was studied in [32]):

$$m_R \bar{\psi}\psi_R / m_\pi^4 = m(\bar{\psi}\psi - \bar{\psi}\psi_0) / m_\pi^4 \quad (3)$$

The renormalized condensate is plotted in Figure 2 together with our staggered estimate. The temperatures are converted to MeV again by using the physical value of  $w_0$ . We can see that there is still some lattice spacing dependence, but the  $N_t = 8$  results are very close to the staggered ones. One observes a broad cross-over, similar to the staggered results at physical quark masses [33].

We have also determined the *chiral susceptibility*

$$\chi_{\bar{\psi}\psi} = (T/V)\partial^2/\partial m^2 \log Z, \quad (4)$$

but at the present level of our statistics renormalization resulted in large errors. Therefore we only show the bare susceptibilities in Figure 3. Even though the results obtained at our two lattice spacings cannot be compared directly, the peaks nicely signal the transition and we can see that the transition temperature defined from this quantity has small lattice spacing dependence.

The next quantity we study is the *Polyakov loop*. The bare quantity has a multiplicative divergence of the form  $\exp[F_0(\beta)/T]$  where the divergent term  $F_0$  can be determined up to a constant [34]. Different constants correspond to different renormalization schemes. We determine  $F_0$  entirely from finite temperature simulations in the following way. We perform runs with six different  $N_t$  values,  $N_t = 4, 5, 6, 7, 8$  and 9, all lattice extents are  $16^3 \cdot N_t$ .

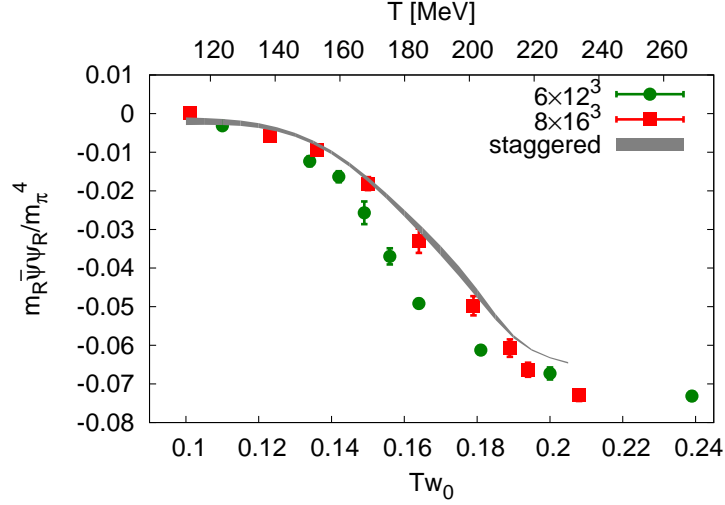


Figure 2: The renormalized chiral condensate as a function of temperature on  $N_t = 6$  and 8 lattices. The upper temperature scale is for illustration only and it is based  $w_0 = 0.1755$  fm [30]. The gray band shows our staggered estimate based on  $N_t = 6, 8$  and 10 simulations. For details see Appendix B.

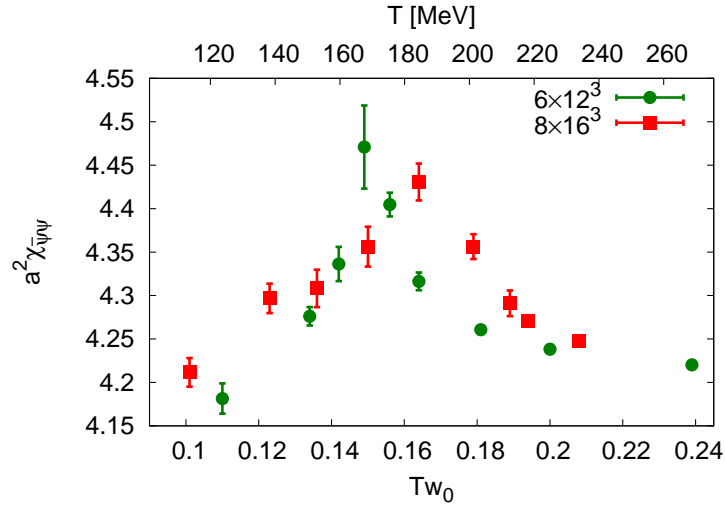


Figure 3: The bare chiral susceptibility as a function of temperature on our  $N_t = 6$  and 8 lattices.

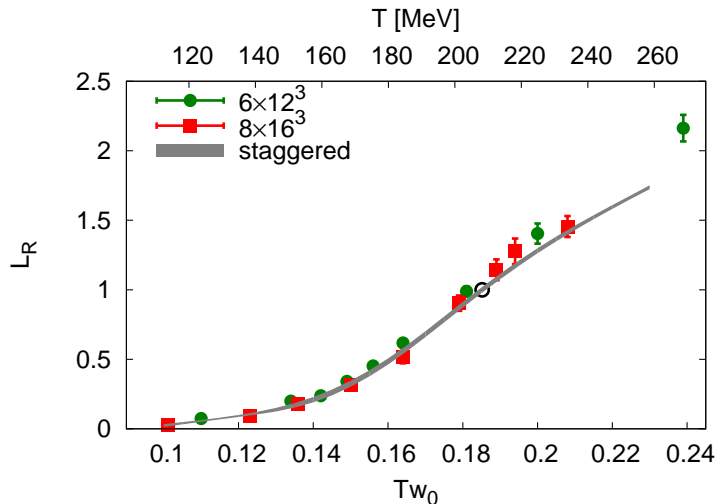


Figure 4: The renormalized Polyakov loop as a function of temperature on  $N_t = 6$  and 8 lattices as well as the staggered result. The black circle represents our renormalization condition,  $L_R(T = 208\text{MeV}) = 1$ .

We choose a fixed physical temperature such that these  $N_t$  values span our  $\beta$  range. This corresponds to a temperature of 208 MeV (having  $N_t = 9$  at  $\beta = 4.1$ ). From these runs we can determine  $F_0(\beta) = 1/N_t \cdot \log L$  at six  $\beta$  values. This can then be extended by interpolation to all of our couplings. This renormalization scheme corresponds to the condition  $L_R(T = 208\text{MeV}) = 1$ . The renormalized Polyakov loop is then given as:

$$L_R = L_0 e^{-N_t \cdot F_0(\beta)}, \quad (5)$$

where  $L_0$  is the bare Polyakov loop. The result is shown in Figure 4. We can see almost no lattice spacing dependence and an excellent agreement with the staggered results.

Our final observable is the *isospin susceptibility*,

$$\chi_I = (T/V) \partial^2 / \partial \mu_I^2 \log Z \Big|_{\mu_I=0}, \quad (6)$$

where  $\mu_I$  is the isospin chemical potential, i.e. the quark chemical potentials are  $\mu_u = \mu_I/2$  and  $\mu_d = -\mu_I/2$ . Obtaining results at non-vanishing chemical potentials is very CPU demanding (see e.g. [35, 36]). Even though our analysis to  $\mu > 0$  is beyond the scope of the present Letter, including the

$N_t$	4	6	8	10	12
$\xi = 2$ overlap	1.700	1.588	1.362	1.241	1.186
$\xi = \infty$ overlap	1.619	1.513	1.290	1.170	1.117
$\xi = \infty$ staggered	2.235	1.861	1.473	1.266	1.164
$\xi = \infty$ Wilson	4.168	2.258	1.521	1.265	1.161

Table 1: Stefan-Boltzmann limits of the quark number susceptibility for three colors of overlap quarks with  $m_0 = 1.3$  for aspect ratios ( $\xi$ ) of 2 and infinity. As a comparison we also give the infinite volume values for Wilson and staggered quarks.

chemical potential even on the level of eq. (6) is quite interesting. The reason is that there is an ongoing discussion in the literature about the proper inclusion of the chemical potential in the overlap operator [37, 38, 39]. We follow Reference [37] and define the chemical potential as a fourth, imaginary component of the temporal gauge field and use the generalization of the sign function:  $\text{sgn}(z) = \text{sgnRe}(z)$ . The second derivative can be calculated using the formulas of Appendix A. As a tree level improvement we normalize all susceptibilities with the corresponding Stefan-Boltzmann (SB) values which, for our choice of  $m_0 = 1.3$  are given in Table 1 for a number of  $N_t$ 's both for infinite volume and our relatively small aspect ratio,  $\xi = 2$ . Our results for the quark number susceptibility are shown in Figure 5. Again, the  $N_t = 8$  results are very close to the staggered ones.

#### 4. Conclusions, outlook

We presented results for the temperature dependence of several observables using dynamical overlap fermions. Our results show that on  $N_t = 6$  and 8 lattices cutoff effects are still present but not severe. The comparison with staggered results obtained on  $N_t = 6, 8$  and 10 lattices is quite encouraging: there is a good chance for a reliable continuum extrapolation from  $N_t \lesssim 10$  lattices with overlap fermions.

There are several remaining issues to investigate in future studies. A particularly interesting question is the dependence of the results on the global topology and how it disappears in the thermodynamic limit. Such analysis requires a series of runs on larger volumes. To approach the continuum limit one needs at least one more lattice spacing. Finally, one might also include the strange quark and decrease the light quark masses to their physical values.



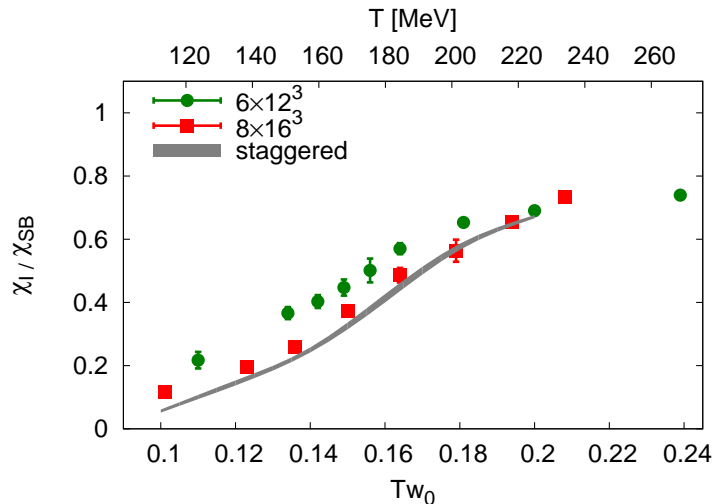


Figure 5: The isospin susceptibility as a function of temperature on  $N_t = 6$  and 8 lattices. The gray band again shows the corresponding staggered result. All data sets were normalized by their corresponding SB limits (cf. Table 1).

## Acknowledgments

Computations were carried out on GPU [40] clusters at the Universities of Wuppertal and Budapest as well as on supercomputers in Forschungszentrum Juelich. This work is supported in part by the Deutsche Forschungsgemeinschaft grants FO 502/2 and SFB- TR 55 and by the EU (FP7/2007-2013)/ERC No. 208740.

## Appendix A. Derivatives of the Zolotarev approximation

Here we present results on the first and second derivatives of the sign function. In the following the  $\delta$  symbol stands for a general derivation operator, for example a derivation with respect to the gauge links or with respect to the chemical potential. The Zolotarev approximation of the sign function of an operator  $h$  can be written in a partial fraction expansion as:

$$\text{sgn}(h) \approx h \left( c_0 + \sum_i \frac{c_i}{h^2 + q_i} \right) = h \left( c_0 + \sum_i c_i Q_i \right), \quad (\text{A.1})$$

where  $Q_i = (h^2 + q_i)^{-1}$  was introduced. The first derivative is

$$\delta \text{sgn}(h) \approx \delta h \left( c_0 + \sum_i c_i Q_i \right) - \sum_i c_i Q_i h \delta h^2 Q_i, \quad (\text{A.2})$$

whereas the second derivative is

$$\delta^2 \text{sgn}(h) \approx \delta^2 h \left( c_0 + \sum_i c_i Q_i \right) + \sum_i Q_i [2\delta h^2 Q_i h \delta h^2 - h \delta^2 h^2 - 2\delta h \delta h^2] c_i Q_i. \quad (\text{A.3})$$

## Appendix B. Details of the staggered calculations

In this appendix we describe our staggered analysis. The sole goal of this study was to provide a basis of comparison for the overlap data. To suppress most of the taste-breaking effects of the staggered action we used four levels of stout smearings ( $\rho = 0.125$ ) in the fermionic sector, which contained here the two light quarks only. We determined a two-flavor LCP for this staggered action using the same definition as in the case of the overlap simulations.

To this end we simulated sixteen ensembles (four lattice spacings with four quark masses each). The smallest mass was always close to the final LCP's value. In the range  $\beta = 3.8 - 4.1$  we could fit the emerging  $am_q(\beta)$  and  $w_0/a(\beta)$  functions to sub-percent accuracy.

For the renormalization of the chiral condensate we made a chiral interpolation (or extrapolation for some lattice spacings) of the vacuum condensate  $\langle \bar{\psi}\psi \rangle_0$ .

The Polyakov loop requires renormalization, too, here we calculated the static potential for our sixteen  $T = 0$  ensembles. One can select any physical distance to remove all divergences. Since  $w_0$  is our most accurately known scale, we used  $\sqrt{8}w_0$  which is around 0.5 fm and defined  $Z = \exp(V(r = \sqrt{8}w_0)/2)$ . After this renormalization our final estimate for the Polyakov loop was multiplied by an  $\exp(-\delta/(w_0 T))$  function, which facilitates finite transformations between different renormalization schemes. We set  $\delta = 0.1566$  to approximately reproduce the renormalization condition used in the overlap results. The renormalization procedure might seem elaborate, yet the dominant source of error comes from our finite temperature statistics.

Our finite temperature simulations were performed with the same aspect ratio as with the overlap action, but here, in addition to  $N_t = 6$  and 8, we

also made a set of  $N_t = 10$  ensembles. In most of the temperature range we had two lattice spacings. The agreement between the results at these lattice spacings was even slightly better than in our previous work in full QCD [34]. For our “staggered estimate” we use the  $N_t = 10$  at low temperatures and we present  $N_t = 8$  data starting from a temperature where both  $N_t = 8$  and 10 data were present and they were in agreement.

## References

- [1] S. Borsanyi, et al., Is there still any  $T_c$  mystery in lattice QCD? Results with physical masses in the continuum limit III, JHEP 09 (2010) 073.
- [2] A. Bazavov, et al., The chiral and deconfinement aspects of the QCD transition, Phys. Rev. D85 (2012) 054503.
- [3] S. Borsanyi, et al., The QCD equation of state with dynamical quarks, JHEP 11 (2010) 077.
- [4] V. G. Bornyakov, et al., Probing the finite temperature phase transition with  $N_f=2$  nonperturbatively improved Wilson fermions, Phys. Rev. D82 (2010) 014504.
- [5] S. Borsanyi, et al., QCD thermodynamics with Wilson fermions (2011).
- [6] T. Umeda, et al., Equation of state in 2+1 flavor QCD with improved Wilson quarks by the fixed scale approach (2012).
- [7] E. M. Ilgenfritz, et al., Phase structure of thermal lattice QCD with  $N_f = 2$  twisted mass Wilson fermions, Phys. Rev. D80 (2009) 094502.
- [8] M. Cheng, et al., The finite temperature QCD using 2+1 flavors of domain wall fermions at  $N_t = 8$ , Phys. Rev. D81 (2010) 054510.
- [9] G. Cossu, et al., Finite temperature QCD at fixed  $Q$  with overlap fermions, PoS LATTICE2010 (2010) 174.
- [10] H. Neuberger, Exactly massless quarks on the lattice, Phys. Lett. B417 (1998) 141–144.
- [11] H. Neuberger, More about exactly massless quarks on the lattice, Phys. Lett. B427 (1998) 353–355.

- [12] M. Luscher, Exact chiral symmetry on the lattice and the Ginsparg-Wilson relation, *Phys. Lett. B*428 (1998) 342–345.
- [13] Z. Fodor, S. D. Katz, K. K. Szabo, Dynamical overlap fermions, results with hybrid Monte- Carlo algorithm, *JHEP* 08 (2004) 003.
- [14] J. van den Eshof, A. Frommer, T. Lippert, K. Schilling, H. van der Vorst, Numerical methods for the QCD overlap operator. I. Sign function and error bounds, *Comput.Phys.Commun.* 146 (2002) 203–224.
- [15] T. A. DeGrand, S. Schaefer, Physics issues in simulations with dynamical overlap fermions, *Phys. Rev. D*71 (2005) 034507.
- [16] N. Cundy, et al., Numerical methods for the QCD overlap operator. IV: Hybrid Monte Carlo, *Comput. Phys. Commun.* 180 (2009) 26–54.
- [17] N. Cundy, S. Krieg, T. Lippert, A. Schafer, Topological tunneling with Dynamical overlap fermions, *Comput. Phys. Commun.* 180 (2009) 201–208.
- [18] G. I. Egri, Z. Fodor, S. D. Katz, K. K. Szabo, Topology with dynamical overlap fermions, *JHEP* 01 (2006) 049.
- [19] H. Fukaya, et al., Lattice gauge action suppressing near-zero modes of  $H(W)$ , *Phys. Rev. D*74 (2006) 094505.
- [20] R. Brower, S. Chandrasekharan, J. W. Negele, U. Wiese, QCD at fixed topology, *Phys.Lett. B*560 (2003) 64–74.
- [21] S. Aoki, H. Fukaya, S. Hashimoto, T. Onogi, Finite volume QCD at fixed topological charge, *Phys.Rev. D*76 (2007) 054508.
- [22] T. G. Kovacs, Locality and topology with fat link overlap actions, *Phys. Rev. D*67 (2003) 094501.
- [23] S. Durr, C. Hoelbling, U. Wenger, Filtered overlap: Speedup, locality, kernel non-normality and  $Z(A) = 1$ , *JHEP* 0509 (2005) 030.
- [24] S. Capitani, S. Durr, C. Hoelbling, Rationale for UV-filtered clover fermions, *JHEP* 0611 (2006) 028. 26 pages, 5 figures.

- [25] S. Durr, et al., Lattice QCD at the physical point: light quark masses, Phys. Lett. B701 (2011) 265–268.
- [26] S. Durr, et al., Lattice QCD at the physical point: Simulation and analysis details, JHEP 08 (2011) 148.
- [27] M. Hasenbusch, Speeding up the Hybrid-Monte-Carlo algorithm for dynamical fermions, Phys. Lett. B519 (2001) 177–182.
- [28] T. Takaishi, P. de Forcrand, Testing and tuning new symplectic integrators for hybrid Monte Carlo algorithm in lattice QCD, Phys. Rev. E73 (2006) 036706.
- [29] J. C. Sexton, D. H. Weingarten, Hamiltonian evolution for the hybrid Monte Carlo algorithm, Nucl. Phys. B380 (1992) 665–678.
- [30] S. Borsanyi, et al., High-precision scale setting in lattice QCD (2012).
- [31] M. Luscher, Properties and uses of the Wilson flow in lattice QCD, JHEP 1008 (2010) 071.
- [32] G. Endrodi, Z. Fodor, S. Katz, K. Szabo, The QCD phase diagram at nonzero quark density, JHEP 1104 (2011) 001.
- [33] Y. Aoki, G. Endrodi, Z. Fodor, S. D. Katz, K. K. Szabo, The order of the quantum chromodynamics transition predicted by the standard model of particle physics, Nature 443 (2006) 675–678.
- [34] Y. Aoki, Z. Fodor, S. D. Katz, K. K. Szabo, The QCD transition temperature: Results with physical masses in the continuum limit, Phys. Lett. B643 (2006) 46–54.
- [35] Z. Fodor, S. Katz, A New method to study lattice QCD at finite temperature and chemical potential, Phys.Lett. B534 (2002) 87–92.
- [36] Z. Fodor, S. Katz, Critical point of QCD at finite T and mu, lattice results for physical quark masses, JHEP 0404 (2004) 050.
- [37] J. C. R. Bloch, T. Wettig, Overlap Dirac operator at nonzero chemical potential and random matrix theory, Phys. Rev. Lett. 97 (2006) 012003.

- [38] R. Gavai, S. Sharma, Anomalies at finite density and chiral fermions, Phys.Rev. D81 (2010) 034501.
- [39] R. Narayanan, S. Sharma, Introduction of the chemical potential in the overlap formalism, JHEP 1110 (2011) 151.
- [40] G. I. Egri, Z. Fodor, C. Hoelbling, S. D. Katz, D. Negradi, et al., Lattice QCD as a video game, Comput.Phys.Commun. 177 (2007) 631–639.